

Regulation by GTP and Its Stable Thiol Derivatives of Calcium Current Components in Rat Nodose Ganglion Neurons

ROBERT A. GROSS, JOHN W. WILEY, THERESE RYAN-JASTROW, and ROBERT L. MACDONALD

Departments of Neurology (R.A.G., T.R.-J., R.L.M.), Physiology (R.L.M.), Internal Medicine (J.W.W.), University of Michigan Medical Center, Ann Arbor, Michigan 48104

Received September 25, 1989; Accepted December 15, 1989

SUMMARY

The calcium current components of acutely dissociated nodose ganglion neurons were characterized using the whole-cell variation of the patch-clamp technique. Many neurotransmitters regulate neuronal calcium currents via GTP binding (G) proteins and in some cases affect calcium current components selectively. To determine whether G proteins regulated these current components in the absence of ligand binding, recording pipettes contained 0.1 mM GTP, guanosine 5'-O-(thiodiphosphate) (GDP- β -S), or guanosine 5'-O-(thiotriphosphate) (GTP- γ -S). Nodose ganglion neurons had three calcium current components, similar to T, N, and L current components found in other sensory neurons. Isolated T currents did not diminish in magnitude during a 20-min recording, but there was a progressive loss of currents containing the N and L current components. The reduction of current magnitude was primarily dependent on the extent of intracellular dialysis and not on the holding potential (V_h) or stimulus frequency. When GDP- β -S was substituted for GTP in the pipette solution, there was no change in the T current or in the rate of run-down of N and L current components. Substitution of GTP- γ -S for GTP in the pipette solution resulted in a moderate

(~40%) loss of isolated T current. This effect was most evident on T currents evoked at relatively positive clamp potentials (V_c , -30 to -15 mV) and occurred relatively late (~10 min) in the recording. In the presence of GTP- γ -S, currents evoked from V_h = -80 mV, containing the N and L current components, were reduced 40-60%, with a lesser effect on those currents evoked from V_h = -40 mV, containing primarily the L current component. The average time to peak current (t_p) was increased 3-4-fold in the presence of GTP- γ -S, and the V_c at which the maximal peak current was evoked was shifted +10 to 20 mV. These effects were evident within 2-5 min after initiation of the whole-cell recording. Pretreatment of neurons with pertussis toxin attenuated or blocked the effects of GTP- γ -S. We conclude that nodose ganglion neurons have T-, N-, and L-type calcium current components, which had different stability during whole-cell recording. Activation of G proteins with GTP- γ -S reduced N > T >> L currents, effects reduced in the presence of pertussis toxin. Thus, the calcium current components of nodose ganglion neurons were regulated by cytosolic constituents and by G $_i$ - or G $_o$ -type G proteins.

Voltage-sensitive calcium channels are primarily gated by changes in membrane potential but are also regulated by a variety of neurotransmitters, including norepinephrine, adenosine, dynorphin A, acetylcholine, neuropeptide Y, and γ -aminobutyric acid (e.g., Refs. 1-6). In most of these cases, the neurotransmitter effects were blocked by PTX, suggesting that G $_i$ - or G $_o$ -type G proteins coupled these receptors to calcium channels (5, 7-9).

Further evidence that G proteins regulate the activity of calcium channels was provided by studies using GTP analogs. GTP- γ -S, a stable thiol derivative of GTP, activates G proteins in the absence of ligand binding (10). In the presence of GTP-

γ -S, calcium currents were reduced in magnitude and activated more slowly, an effect similar to that observed with neurotransmitters (see, e.g., Refs. 11 and 12). In contrast, GDP- β -S, which binds to but does not activate G proteins, had little effect on calcium currents but blocked the effect of certain neurotransmitters (e.g., Refs. 5 and 7). G proteins, or their α subunits, also regulate calcium channel activity. In heart cells, channel activity was enhanced in the presence of GTP- γ -S-activated α_s subunits (13). G $_o$ or α_o "reconstitutes" the effect of neuropeptide Y (8) or opioid peptides (14) on calcium currents in cells previously treated with PTX.

Previous work from this laboratory showed that certain neurotransmitters can differentially regulate calcium current components of cultured dorsal root ganglion neurons and that, in at least one case (2-chloroadenosine), this selective reduction of a calcium current component was mediated by a PTX-

This work was supported in part by National Institutes of Health Grants NS01019 and NS19613 to R.A.G., DA04122 to R.L.M., and DA05345 to T.R.-J. and a Veteran's Administration Research Associate Award and an American Gastroenterological Association Industry Scholar Award to J.W.W.

ABBREVIATIONS: G protein, GTP-binding protein; PTX, pertussis toxin; GTP- γ -S, guanosine-5'-O-(3-thio)triphosphate; GDP- β -S, guanosine-5'-O-(2-thio)diphosphate; EGTA, ethylene glycol bis(β -aminoethyl ether)-N,N,N',N'-tetraacetic acid; HEPES, 4-(2-hydroxyethyl)-1-piperazineethanesulfonic acid.

sensitive G protein (4, 9). The above-mentioned studies showed that GTP analogs and/or G protein subunits can directly affect calcium currents or channel activity in the absence of ligand binding. The specific effects of G proteins on the T-, N-, or L-type calcium current components (15–17) are not yet fully described, however, nor are the mechanism(s) by which the currents are affected. Such studies could provide insight into the mechanisms that couple receptors to calcium channels.

We, therefore, undertook this study to characterize the effect of GTP and its stable thiol derivatives on the calcium current components of acutely dissociated nodose ganglion neurons. We recorded currents using the whole-cell variation of the patch-clamp technique and found that the three calcium current components had differential stability during whole-cell "dialysis." As a result, we examined the effects of GTP, GTP- γ -S, and GDP- β -S as a function of time after patch rupture, to control for time-dependent changes in the effects of GTP or its analogs. In addition, we used PTX to determine that the observed effects were mediated by G_i - or G_o -type G proteins.

Materials and Methods

Preparation of acutely dissociated neurons. Nodose ganglion neurons were prepared from 6–10-day-old rats, using a procedure modified from that of Ikeda *et al.* (18). The ganglia were removed and placed in oxygenated Ca^{2+} - and Mg^{2+} -free buffer (D₁SGH or Dulbecco's phosphate-buffered saline) in a culture dish on ice. After the dissections, the ganglia were transferred to a tube containing 0.5 ml of collagenase/ganglion (1 mg/ml in Ca^{2+} - and Mg^{2+} -free buffer; Sigma Chemical Company, St. Louis, MO) and incubated for 10 min at room temperature. An aliquot of buffer containing bovine serum albumin and fetal calf serum was added to inhibit the enzyme (to final concentrations of 1 mg/ml and 5%, respectively). The ganglia were triturated gently 10 times to disperse the cells, and the mixture was centrifuged at $\sim 500 \times g$ for 10 min. The pellet was resuspended in minimum essential medium with Earle's salts (GIBCO Laboratories, Grand Island, NY) supplemented with $NaHCO_3$ (16.5 mM), glucose (28.2 mM), nerve growth factor (10 ng/ml), penicillin (50 units/ml), streptomycin (50 mg/ml), $CaCl_2$ (3.6 mM), and 10% fetal calf serum. The suspension (approximately 0.5 ml/ganglion) was plated 0.3 ml/dish and incubated at 37°, and an additional 1 ml of medium was added after 30 min.

Whole-cell patch-clamp recordings. Whole-cell voltage-clamp recordings were obtained using the whole-cell variation of the patch-clamp technique. Glass recording patch pipettes with resistances of 1–2 M Ω were filled with a recording solution of the following (in mM): 140 CsCl, 10 HEPES, 10 EGTA, 5 ATP- Mg^{2+} , and 0.1 GTP, GTP- γ -S-Li, or GDP- β -S-Li (Sigma). The pH was adjusted to 7.2–7.3 with CsOH and the osmolality to 10–15% below that of the bath solution (280–300 mOsm). Cells were bathed in a solution of the following (in mM): 67 choline chloride, 100 tetraethylammonium, 5.6 glucose, 5.3 KCl, 5.0 $CaCl_2$, 0.8 $MgCl_2$, and 10 HEPES (pH 7.3–7.4, 310–330 mOsm). Under these conditions, sodium and potassium currents were virtually eliminated; evoking currents in the presence of 200 μM Cd^{2+} eliminated the inward currents, with no evidence of outward currents at V_c as positive as +30 mV (data not shown).

Recordings were made 2–8 hr after plating, before the outgrowth of processes, at room temperature using the Axopatch 1-B patch-clamp amplifier (Axon Instruments, Burlingame, CA). Pipette and whole-cell capacitances were corrected using compensation circuitry on the amplifier. Initial input resistances were 500 M Ω to 1 G Ω and series resistance was typically 2–5 M Ω . In most cases, series resistance compensation of 80–90% was possible without significant noise or oscillation.

Voltage step commands were generated, and the evoked currents were digitized (at 1.6–5 kHz), stored, and analyzed by a microcomputer (IBM AT or equivalent) using the program pClamp (Axon Instru-

ments). The current traces were filtered with a Bessel filter at 10 kHz (–3 dB).

Analysis of current components. Leak currents were estimated by using hyperpolarizing voltage commands of equal magnitude to the depolarizing commands used to evoke the inward currents. The resulting current was assumed to be equal and opposite in magnitude to the leak current and was digitally subtracted from the relevant inward current to obtain the calcium current. If the current evoked during the hyperpolarizing command was not constant over time, that current was not included in the analyses.

Three calcium current components were recorded from acutely dissociated nodose ganglion neurons. Given the differences in recording technique, temperature, and charge carrier, the recorded currents were similar to T, N, and L currents described in chick and cultured mouse dorsal root ganglion neurons (15–17; 4, 9, 19). The major differences from the latter studies, which used the single-electrode voltage-clamp technique at 35°, were that, in the present experiments, the voltage ranges for current activation and inactivation were shifted towards more positive potentials and that current activation and inactivation were slower. The former differences were most likely due to changes in the concentration of Ca^{2+} in the bathing medium and the latter to the difference in temperature (data not shown).

The T current was present in the majority of nodose neurons tested (~95%), although the magnitude varied greatly (in cells of similar size), between 0.2 and 2.0 nA (evoked from V_h of –90 to –80 mV at V_c of –25 to –15 mV). At V_c positive to –15 mV, a current component was evident that had a slower inactivation rate (see below). Maximal T currents were defined as those evoked at V_c negative to those at which a more slowly inactivating current component was evoked.

We used $V_h = -40$ mV to evoke currents that consisted primarily of the L current at V_c at or positive to +10 mV. Using this paradigm, a slowly activating and inactivating current was evoked. At this V_h , there was no clear T current component, but in some neurons we observed a more rapidly activating and inactivating component that probably represented residual N current. Also, some L current was inactivated in the steady state at this V_h .

When currents were evoked from $V_h = -80$ mV, an additional current component was evoked. The N current component activated and inactivated more rapidly than the L current component. By comparing currents evoked at the same V_c from V_h of –80 and –40 mV, an estimate of the N current component was possible.

The present data were obtained from approximately 150 neurons over a 6-month period.

Statistical comparisons. Statistical comparisons were made using Student's two-tailed *t* test.

Results

Nodose ganglion neurons had three calcium current components with differential stability during whole-cell recording. In the first series of experiments, we characterized the calcium current components of acutely dissociated rat nodose ganglion neurons and determined their stability during whole-cell recording. T currents were studied by evoking a series of currents from V_h of –90 or –80 mV at V_c ranging from –65 to –5 mV in 5-mV increments (Fig. 1). T currents were evoked at V_c at or positive to –55 mV (Fig. 1, A and B), with the maximal T current occurring at V_c of –25 to –15 mV. In some but not all neurons, the V_c at which T currents were evoked shifted approximately –5 mV during the recording period (Fig. 1B). T current was very stable, with no "run-down" evident during a 15–20-min recording (compare Fig. 1, A1 and A2 with C).

We next studied the current components evoked at V_c positive to those which evoked T currents (Fig. 2). In neurons held at $V_h = -90$ mV, maximal currents were evoked at V_c of –10

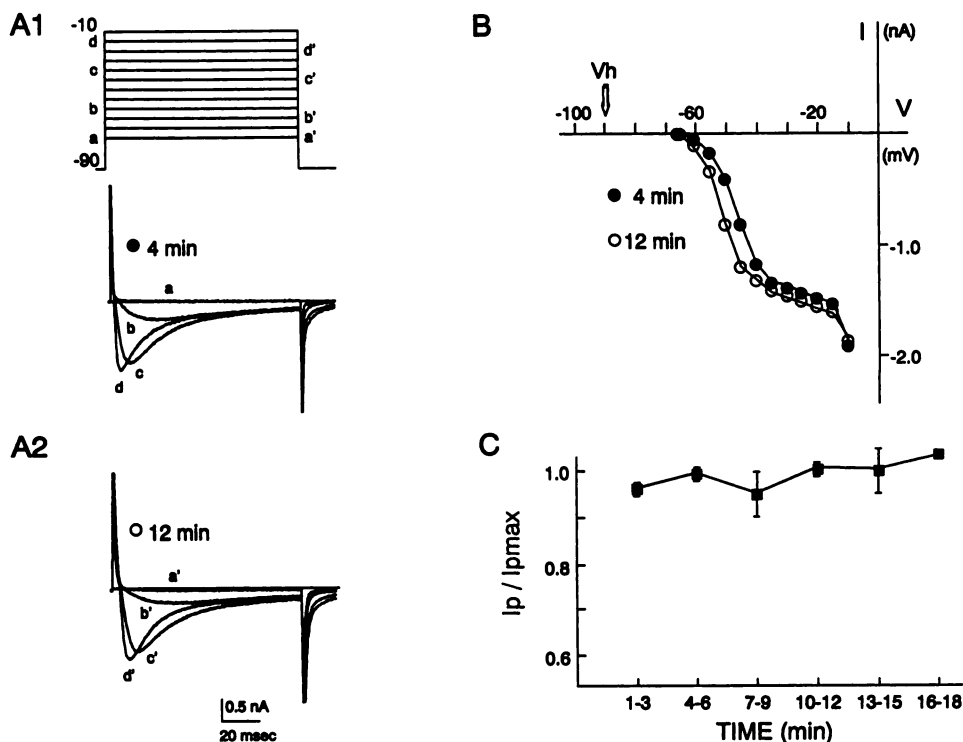
GTP $100 \mu\text{M}$ 

Fig. 1. T currents in control nodose ganglion neurons during whole-cell recording. In this and other figures, currents are leak subtracted unless otherwise noted. Inward currents are downward. Holding potentials (V_h) and clamp potentials (V_c) are stated or are shown as part of an illustrative voltage command. T currents were evoked every 1–3 min from $V_h = -90$ mV by a series of 100-msec commands in 5-mV increments. The recording pipette contained the standard solution, including 0.1 mM GTP. Two abbreviated series of currents from one neuron are shown 4 min (A1 and B) (●) and 12 min (A2 and B) (○) after patch rupture, as are peak current-voltage relation plots (B), derived from the complete series of currents. In this neuron, there was a slight shift (–5 mV) of the current-voltage relation during the recording. The peak current magnitudes (I_p) of the maximum T current from each series were normalized to the peak T current occurring in the first 5 min of the recording ($I_{p_{max}}$). Similar data from six neurons were pooled and sorted into 3-min epochs (C). The symbols show the mean normalized current magnitudes \pm standard error. T current magnitude did not change in control neurons during whole-cell recording.

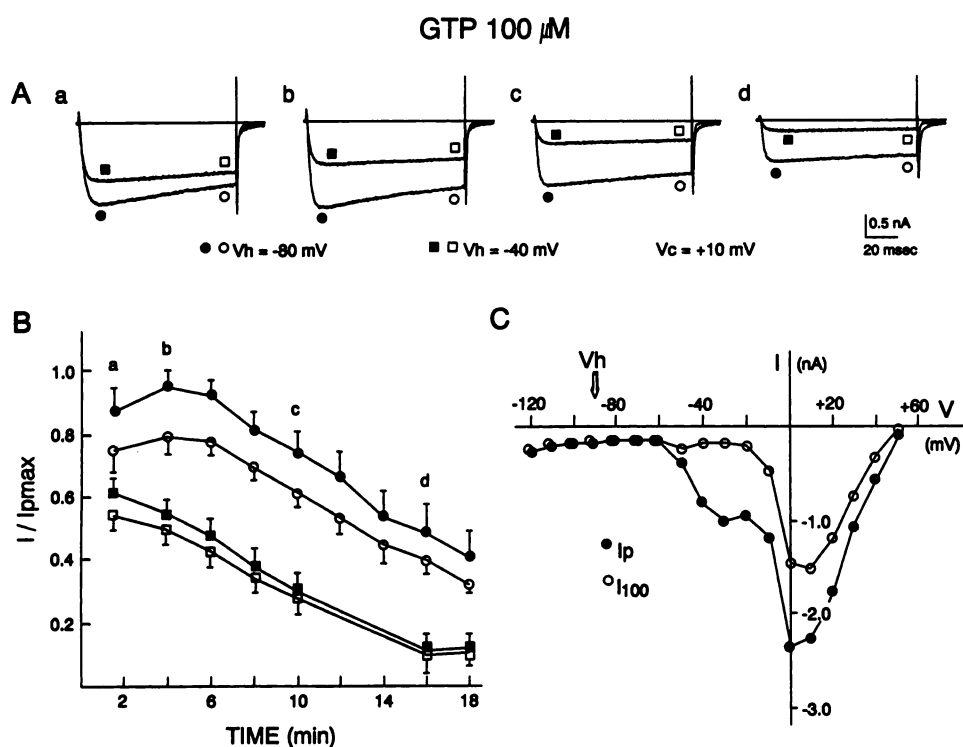


Fig. 2. N and L current components in control neurons. Control currents were evoked with 100-msec voltage commands at $V_c = +10$ mV every minute after patch rupture, alternating between $V_h = -80$ mV (circles) and -40 mV (squares). Pairs of calcium currents are shown, recorded from a single control neuron, at 1–2, 3–4, 9–10, and 16–17 min (A, a–d, respectively) after patch rupture. The I_p and I_{100} values (closed and open symbols, respectively) from 11 neurons were normalized to the maximal peak current occurring within the first 5 min of the recording ($V_h = -80$ mV; $I_{p_{max}}$). The values were sorted into 2-min epochs and plotted as a function of time after patch rupture (B). The symbols show the mean current magnitude in each epoch for 3–11 currents from the 11 neurons (\pm standard error; error bars shown in one direction only). There was an initial increase in the current evoked from $V_h = -80$ mV (a and b) and then a steady decline (b–d); the current evoked from $V_h = -40$ mV declined throughout the recording. In other neurons, currents were evoked every 10 sec with 100-msec hyperpolarizing and depolarizing voltage commands from a $V_h = -90$ mV at V_c of -120 to $+50$ mV. I_p and I_{100} values were plotted to obtain the current-voltage relations (C). T current was evoked at V_c of -50 to -20 mV, and the maximal I_p was found at -10 to 0 mV. I_{100} was evoked at or positive to -10 mV, with a maximum value at $V_c = 0$ to $+10$ mV.

to 0 mV, a voltage range distinct from that of the T current. Current-voltage plots (Fig. 2C) comparing peak current (I_p) and late current (I_{100}) values showed that maximal I_{100} values were achieved at slightly more positive V_c , about +10 mV.

In order to study the N and L current components in more detail, we compared currents evoked at $V_c = +10$ mV from V_h of -80 and -40 mV, evoked alternately at 1-min intervals (see Materials and Methods; Fig. 2). The maximal current was attained 3–5 min after patch rupture (see Fig. 2A, traces a–d). Thereafter, the currents steadily declined. To quantitate this, we normalized current amplitudes to the maximal I_p of currents evoked from $V_h = -80$ mV ($I_{p_{max}}$). For example, 17–18 min after patch rupture, currents evoked from $V_h = -80$ mV had declined to $42.0 \pm 5.0\%$ (mean \pm SE, $n = 18$) of $I_{p_{max}}$ (Fig. 2B). Currents evoked from $V_h = -40$ mV, initially $63.4 \pm 2.5\%$ of $I_{p_{max}}$ ($n = 10$), declined to $11.5 \pm 0.9\%$ of $I_{p_{max}}$ ($n = 4$).

The rate of current run-down was variable among neurons but was greater when lower resistance recording pipettes were used. Conversely, when higher resistance electrodes were used (3–5 M Ω), currents stabilized more slowly and declined at a slower rate. Current run-down was not simply due to accumulation of inactivation; currents evoked at 5-min intervals from $V_h = -80$ mV showed the same rate of current decline as described above when electrodes of similar resistance were used (data not shown).

These initial experiments showed that T currents, evoked at relatively negative V_c , were very stable during whole-cell recordings. In contrast, currents containing the N and L components were evoked at more positive V_c , and progressively declined throughout the recordings.

Thiol derivatives of GTP had different effects on calcium current components of nodose neurons. In the next series of experiments, we examined the effects of substituting GDP- β -S or GTP- γ -S for GTP in the recording pipette. In the presence of GDP- β -S, T currents were similar to those evoked in the presence of GTP (Fig. 3, A1 and A2); the current-voltage relations were similar to those in control neurons (Fig. 3A3) and there was no change in I_p during the recording (Fig. 3A4). In the presence of GTP- γ -S, initial T current magnitudes tended to be smaller than those in control neurons, although the difference did not reach statistical significance (0.53 ± 0.1 nA, $n = 7$ and 0.79 ± 0.17 nA, $n = 6$, respectively; $p > 0.05$). In contrast to control T currents, however, T currents in the presence of GTP- γ -S declined in magnitude to about 60% of maximal I_p values (Fig. 3, B1 and B2). This effect was evident 8–10 min after patch rupture (Fig. 3B4). In addition, the reduction in T current was often, but not always, evident at more positive V_c (Fig. 3B3). In all cases, T current magnitudes were measured at V_c negative to those at which slower inactivating current components appeared.

GDP- β -S had no effect on N and L current components (Fig. 4, A1 and A2), compared with those evoked in the presence of GTP. In the presence of GTP- γ -S, however, these current components differed from those evoked in the presence of GDP- β -S or GTP. I_p was reduced, an effect evident within the first minutes of the recording (Fig. 4, B1 and B2). In one series of experiments, for example, the $I_{p_{max}}$ in control neurons, evoked at $V_c = +10$ mV, was 2.82 ± 0.25 nA (mean \pm SE, $n = 18$); in the presence of GTP- γ -S, the $I_{p_{max}}$ was 1.3 ± 0.2 nA ($n = 9$; $p < 0.01$). $I_{p_{max}}$ also occurred sooner after patch rupture in the

presence of GTP- γ -S, 1.7 ± 0.3 min ($n = 9$), compared with 2.8 ± 0.4 min ($n = 18$) in controls ($p < 0.05$).

The rate of current activation was also slowed in the presence of GTP- γ -S. In control neurons, the I_p of currents evoked at $V_c = +10$ mV from $V_h = -80$ mV occurred ~ 14 msec after the onset of the depolarizing voltage command and ~ 22 msec when currents were evoked from $V_h = -40$ mV (Fig. 2A and 5D). In the presence of GTP- γ -S, the I_p occurred at ~ 55 msec ($V_h = -80$ mV) and ~ 80 msec ($V_h = -40$ mV) (Figs. 4B1 and 5D).

The extent of current run-down in the presence of GDP- β -S was similar to that of controls (Fig. 4A1). Run-down was more rapid in the presence of GTP- γ -S (Fig. 4B1), however, an effect which was greater for currents evoked from $V_h = -80$ mV. There was little change in the rate of current run-down for currents evoked from $V_h = -40$ mV in the presence of GTP- γ -S (compare Fig. 2B and 4B1). In addition, there was little inactivation during the 100-msec depolarizing commands (compare differences between I_p and I_{100} values in Fig. 2B, 4A1 and 4B1). That is, GTP- γ -S slowed the activation and reduced the magnitude of calcium currents containing both N and L components, but this effect was greater on currents evoked from $V_h = -80$ mV.

There was no effect of GDP- β -S on the current-voltage relation. As in control neurons, T currents were evoked at V_c of -50 to -20 mV; the maximal I_p was evoked at V_c of -10 to 0 mV and the maximal I_{300} was evoked at V_c of 0 to +10 mV (Fig. 4A2). In the presence of GTP- γ -S, the T current was evoked over a similar range of V_c , but the maximal I_p was evoked at more positive V_c , 0 to +20 mV, a range similar to that of I_{300} evoked in control or GDP- β -S-treated neurons (Fig. 4B2).

Pertussis toxin attenuated the effect of GTP- γ -S. Because GTP- γ -S binds to all subtypes of G proteins, we performed the following experiment to determine the class of G proteins mediating the GTP- γ -S effect on calcium currents. Neurons were pretreated with PTX (150 ng/ml) for 4–8 hr at 37° before recordings were made. We also included PTX (100–150 ng/ml) in the recording pipette.

Using this method, we found that PTX attenuated or reversed the effect of GTP- γ -S on calcium currents (Fig. 5). $I_{p_{max}}$ in the presence of GTP- γ -S plus PTX, 2.3 ± 0.4 nA (mean \pm SE, $n = 7$), was similar to the $I_{p_{max}}$ in control neurons, 2.82 ± 0.25 nA ($n = 18$) (Fig. 5C). Furthermore, the time to I_p was the same as in controls, ~ 13 msec ($V_h = -80$ mV) (Fig. 5D). In neurons from which recordings could be obtained for longer than 15 min, there was a slight increase in the time to I_p , suggesting that, despite the presence of PTX in the recording pipette, GTP- γ -S was having an effect on calcium currents.

PTX may have partially reversed the effect of GTP- γ -S on T current, but this effect was less pronounced than the effect on the N and L current components. The $I_{p_{max}}$ values were similar in the presence of GTP- γ -S (0.52 ± 0.1 nA; $n = 7$) and GTP- γ -S plus PTX (0.51 ± 0.1 nA, $n = 7$). At 10–12 min after patch rupture, T current had declined to $\sim 80\%$ of $I_{p_{max}}$ values in the presence of GTP- γ -S plus PTX (data not shown), compared with $\sim 60\%$ in the presence of GTP- γ -S only (Fig. 3).

Discussion

Calcium current components had differential stability during whole-cell recording. Nodose ganglion neurons had

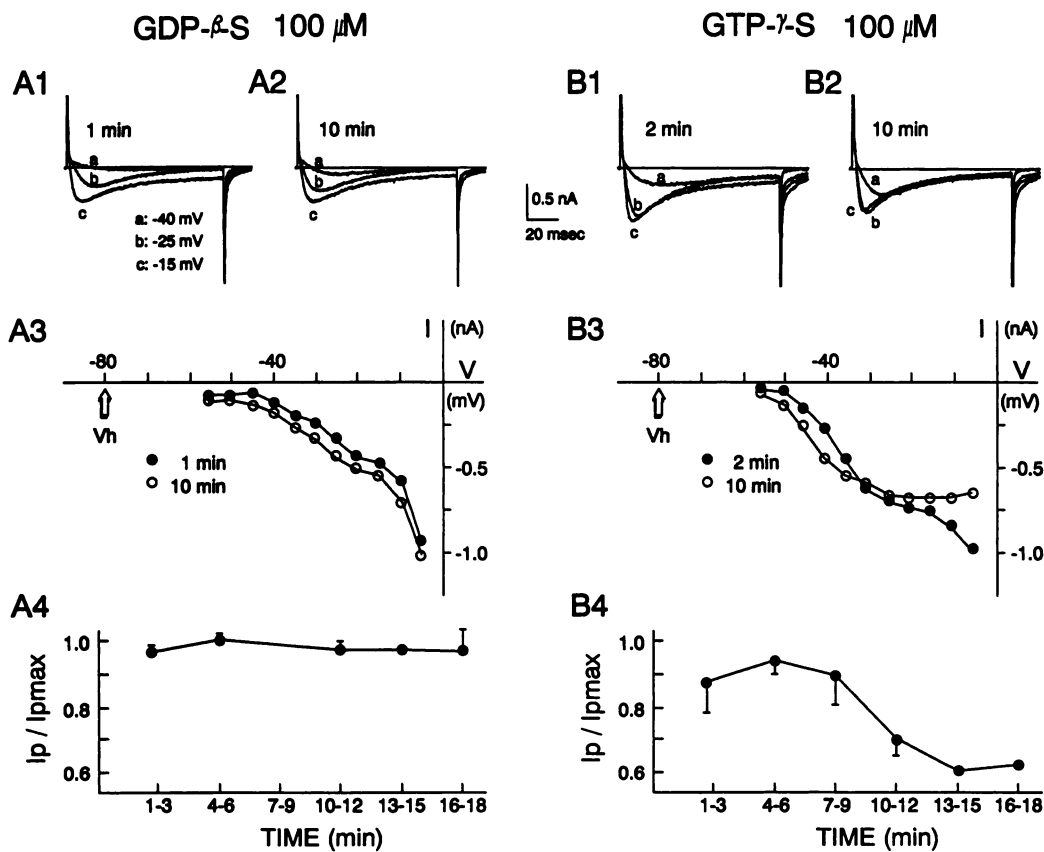


Fig. 3. GDP- β -S and GTP- γ -S effects on the T current. T currents were evoked using a series of 100-msec voltage commands from $V_h = -80$ mV at $V_c = -65$ to -10 mV. The recording pipette contained the standard solution, except that either 0.1 mM GDP- β -S (A) or 0.1 mM GTP- γ -S (B) was substituted for GTP. T currents from two neurons are shown, recorded 1–2 (A1 and B1) and 10 (A2 and B2) min after patch rupture. The V_c were -40 , -25 , and -15 mV (traces a–c). I_p values were used to construct current-voltage relation plots (A3 and B3). There was no effect of GDP- β -S on the T current-voltage relation, compared with controls (compare with Fig. 1B), but GTP- γ -S reduced the magnitude of T currents, especially at the more positive V_c . [Note also that, in the presence of GTP- γ -S, the additional current component (N) evoked at more positive V_c was not present later in the recording.] Maximal I_p values from five to seven neurons were pooled and sorted into 3-min epochs (A4 and B4). T currents were stable in the presence of GDP- β -S, but in the presence of GTP- γ -S T currents were reduced in magnitude, especially 6–8 min after patch rupture. The values show the mean \pm standard error of three to seven I_p values; error bars are not shown if they fall within the symbol and otherwise in one direction only.

three different calcium current components, similar to those first described in chick dorsal root ganglion neurons (15) and subsequently described by other investigators (4, 5, 20–22). The T current had a distinct voltage range of activation, whereas those for N and L currents partially overlapped, the N current having the more negative voltage range. For example, maximal peak and late current values were reached at different V_c (Fig. 2C and 4A2). This is consistent with the idea that these currents contained two current components, which are in different proportions at I_p and I_{300} ; the N current component, inactivating more rapidly than the L current component, comprised a greater proportion of I_p than of I_{300} . In addition, the N current component was present in a greater proportion in currents evoked from $V_h = -80$ mV, whereas the L current component was predominant in currents evoked from $V_h = -40$ mV.

These calcium current components had differential stability during whole-cell recording. T currents were stable throughout the duration of a typical recording, about 20 min. In contrast, currents containing the N and L current components, evoked from either $V_h = -80$ or -40 mV, declined during the recording period. The instability of the current evoked from $V_h = -40$ mV during whole-cell recording is consistent with results in other preparations, in which L-type currents “run down” after the initiation of intracellular dialysis or after excision of a membrane patch (e.g., Refs. 23–25). The loss of the inactivating current component during the recording (i.e., the difference

between I_p and I_{100} declined throughout the recording period) suggests that the N current component was as unstable as the L current component.

We, therefore, conclude that, unlike T currents, neither N nor L current components were stable during recordings using the whole-cell technique. Because run-down was slower with higher resistance recording pipettes, current run-down was more likely related to the extent of intracellular “dialysis” than to changes in V_h or to a high stimulus frequency. This hypothesis is supported by a recent report describing reversal of cardiac myocyte calcium channel run-down by tissue extract (26). In other preparations, calcium currents have been stabilized by including ATP, cyclic AMP, and/or ATP-regenerating systems (23–25, 27). In our experiments using nodose ganglion neurons, calcium currents were slightly less stable without ATP in the recording pipette. Other diffusible factors are presumably lost, therefore, which maintain calcium channels in activatable states. Preliminary experiments from this laboratory show that the catalytic subunit of the cyclic AMP-dependent protein kinase can prevent the run-down of the N and L current components (28).

GTP- γ -S, but not GDP- β -S, differentially affected calcium current components in a pertussis toxin-sensitive manner. Recent work from this and other laboratories has shown that several neurotransmitters that regulate voltage-dependent calcium channels do so via G proteins (e.g., Refs. 5,

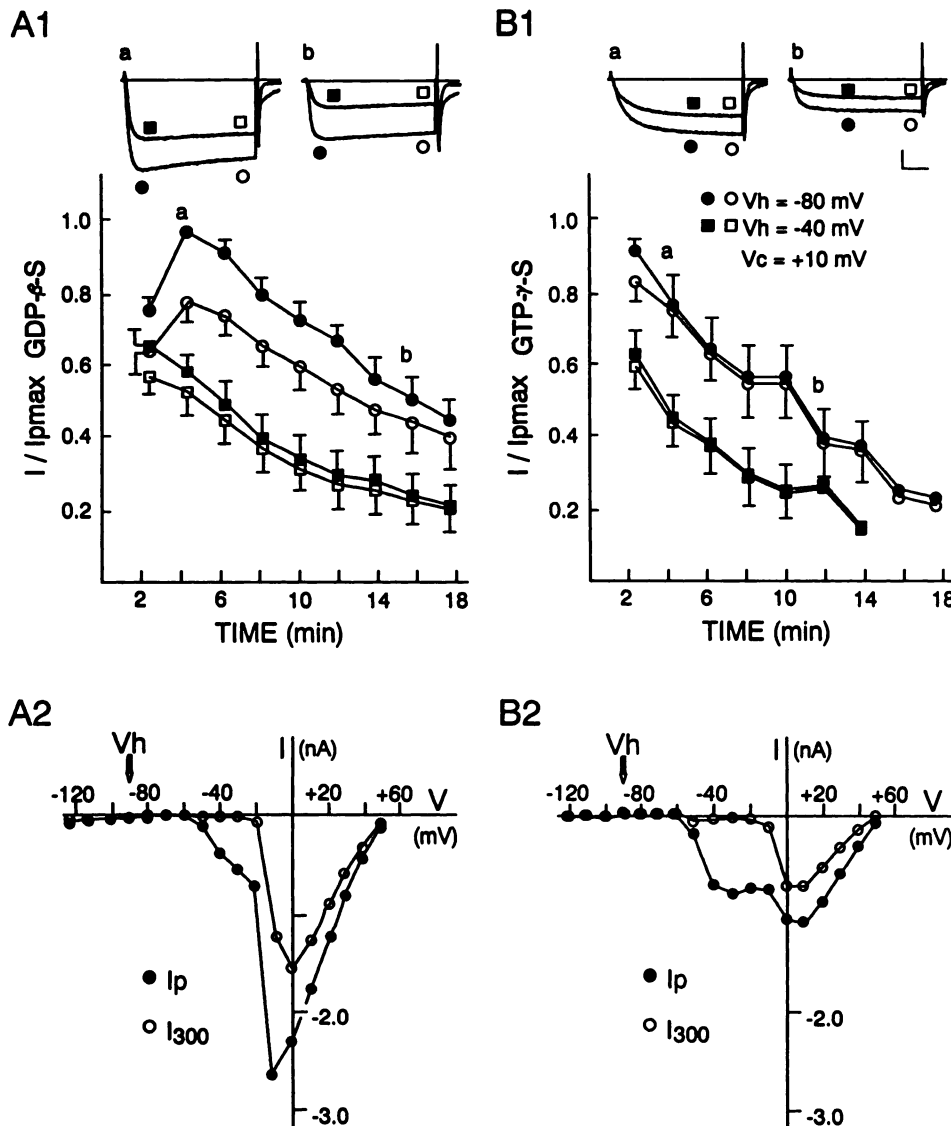
GDP- β -S 100 μ MGTP- γ -S 100 μ M

Fig. 4. GDP- β -S and GTP- γ -S effects on currents containing the N and L current components. Currents were evoked every minute after patch rupture with 100-msec voltage commands to +10 mV, alternating between $V_h = -80$ mV (circles) and -40 mV (squares), in the presence of GDP- β -S (A) and GTP- γ -S (B). Pairs of calcium currents are shown from two different neurons, recorded at 3–4 and 15–16 min (A1, a and b) or 3–4 and 12–13 min (B1, a and b) after patch rupture. Currents were unaffected by GDP- β -S, compared with controls, but in the presence of GTP- γ -S currents were smaller and activated at a slower rate (note position of symbols). Calibration bars indicate 0.5 nA (vertical) and 20 msec (horizontal). I_p (closed symbols) and I_{300} (open symbols) values were pooled from six (GDP- β -S) or eight (GTP- γ -S) neurons and sorted into 2-min epochs (A1 and B1, bottom). The time course of currents recorded in the presence of GDP- β -S was similar to that of controls. In the presence of GTP- γ -S, currents diminished at a more rapid rate, especially those evoked from $V_h = -80$ mV. In addition, there was little difference between the I_p and I_{300} values in the presence of GTP- γ -S. The symbols represent the means \pm standard errors of three to eight current magnitudes at each time point; error bars are shown in one direction only. Corresponding current-voltage relation plots (A2 and B2) were derived from currents recorded about 9 min after patch rupture. GDP- β -S had little effect on the inward current-voltage relation (A2), compared with controls. There was little effect of GTP- γ -S on the T current-voltage relation, but the N and L current components activated at more positive V_c (B2); I_p and I_{300} reached maximum values at the same relatively positive V_c , about +10 mV.

7, and 9). To study the regulation of calcium current components by G proteins in more detail, we used the stable thiol derivatives of GTP to alter G protein function in the absence of ligand binding. By studying currents as a function of time after patch rupture, we were able to control for time-dependent changes in the current components and for any possible time-dependent changes in the effects of the GTP analogs on those current components. GDP- β -S had no effect on the T, N, or L current components. GTP- γ -S reduced the magnitude of the T current and, to a greater extent, the magnitude of currents containing the N and L components. In addition, the rate of current activation of the latter currents was slowed. These effects confirm those of other laboratories (e.g., Refs. 5, 12, and 13).

In the presence of GTP- γ -S, there was a decline in T current magnitude seen after several minutes of recording. It is not clear from the present experiments why this effect had such a long "latency," because recent experiments using caged GTP- γ -S (photolysis activated) suggest that this effect is rapid in

onset (13). It is unlikely that several minutes were required for delivery of GTP- γ -S from the recording pipette to the intracellular space, because the effect on N/L currents was evident within the first 1–2 min of whole-cell recording. The effect of GTP- γ -S was also more pronounced when T currents were evoked at relatively positive potentials ($V_c = -30$ to -15 mV); this suggests that GTP- γ -S may affect a voltage-sensitive process such as channel gating. Alternatively, it is possible that a non-T current component, evoked at these V_c , was affected rather than T currents.

The effect of GTP- γ -S was greater for currents evoked from $V_h = -80$ mV than for those evoked from $V_h = -40$ mV. The difference between the I_p values of currents evoked from $V_h = -80$ and -40 mV was smaller in the presence of GTP- γ -S than for control currents (see Fig. 4). In addition, the maximal I_p of the current-voltage relation was shifted +10–20 mV relative to control and was very similar to the late current-voltage relation. These results, taken together, suggest either that the N current component was reduced or eliminated in the presence of GTP-

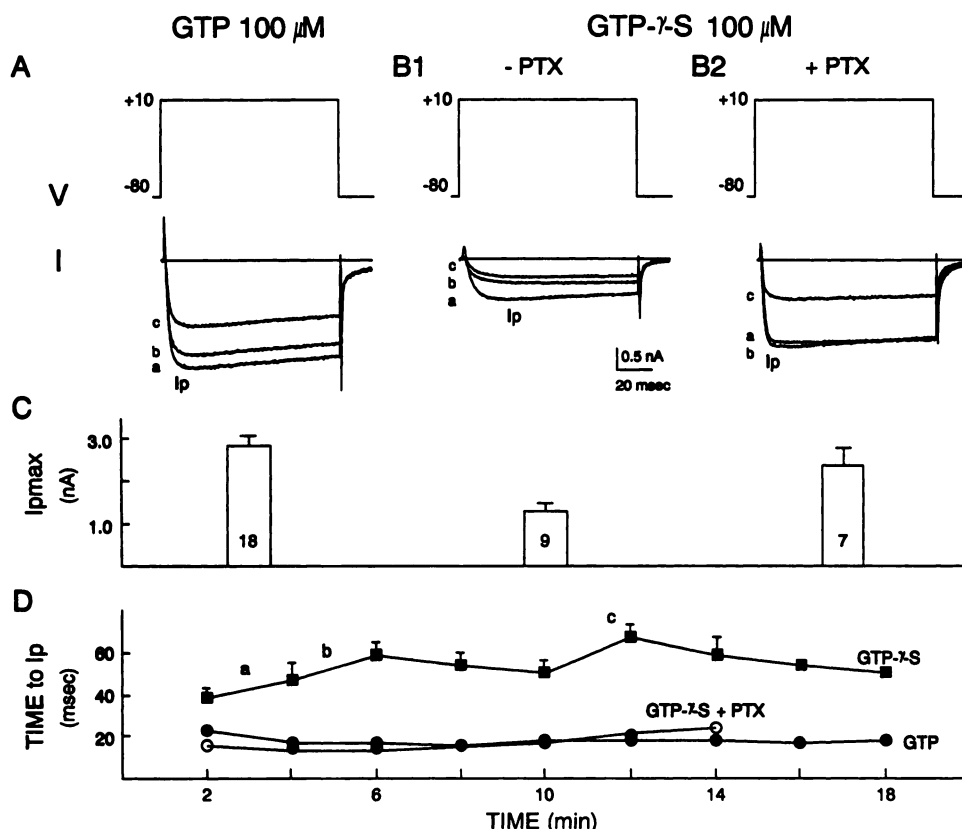


Fig. 5. Calcium currents in the presence of GTP, GTP- γ -S, and GTP- γ -S plus PTX. Currents were evoked from $V_h = -80$ mV at $V_c = +10$ mV at 1-min intervals after patch rupture. Some neurons were pretreated with PTX (100–150 ng/ml) for 4–8 hr (B2) before recordings were made. Recording pipette solutions contained 0.1 mM GTP (A) or GTP- γ -S (B1 and B2); in those neurons pretreated with PTX, the recording pipette also included PTX (100–150 ng/ml). Calcium currents from three neurons are shown, each with three superimposed currents recorded between 3 and 11 min after patch rupture (traces a–c). PTX prevented the reduction of current magnitude (C) and the slowing of activation (D) produced in the presence of GTP- γ -S. Values shown in C and D are the means \pm standard errors of the number of neurons shown in C. Error bars are shown in one direction only. In D, error bars are shown only if they fall outside the symbol.

γ -S or that the voltage dependency of current activation was altered so as to become similar to that of the L current component, or both.

The slowing of the rate of current activation probably indicates that the gating properties of calcium channels were different as a result of an action of GTP- γ -S but does not eliminate the possibility that the channels were converted to an inactivated state as well. In a recent report, Bean (29) suggested that the slowed activation of calcium currents by neurotransmitters (and presumably by GTP- γ -S as well) may be due to a shift in the voltage-dependence of channel activation to more positive potentials.

Further studies will be required, using single-channel current analysis, to identify unambiguously the calcium channels associated with the current components described here and the mechanisms by which GTP- γ -S affects channel gating.

The effects of GTP- γ -S were PTX sensitive. Because PTX stabilizes the α subunit of G proteins in the inactivated (GDP-bound) state (30), it slows or prevents subsequent binding of GTP and presumably of GTP- γ -S. Thus, the ability of PTX to attenuate or block the effect of GTP- γ -S on calcium currents supports the idea that these actions were mediated by G_i - and/or G_o -type G proteins. The present studies do not, however, allow us to distinguish between the possibilities that G protein activation directly affected calcium channel function and that it did so indirectly by modulating the activity of a second messenger system. Recent evidence suggests G proteins may directly regulate calcium channel activity (14), but further study will be required to resolve this issue.

A variety of neurotransmitters affect neuronal calcium currents via PTX-sensitive G proteins (see Introduction); in some

cases, only the N current component is affected (4, 5, 9, 29). It is significant, therefore, that GTP- γ -S may preferentially reduce the N current component in sensory neurons, an effect that was presumably mediated through the same G protein subtypes but independent of receptor binding. Other G proteins are also activated by GTP- γ -S, however. Thus, the present studies suggest that the effect of G_i / G_o -type G proteins is predominant over other G protein-mediated effects but do not eliminate the possibility that other G protein-dependent pathways (e.g., second messenger systems) (31–33) modulate calcium channel activity. In a given neuron, therefore, the modes of regulation of calcium-dependent processes would depend on the complement of extracellular neurotransmitter receptors and their associated G protein subtypes, their linkage to calcium channels or second messenger systems, and the interactions of these various pathways. If, as has been suggested, calcium channel subtypes have different roles in neuronal function (34, 35), then certain classes of G proteins, by affecting specific channel subtypes, may be responsible for regulating discrete neuronal processes such as neurotransmitter release.

Acknowledgments

The authors thank Ms. Nancy Fox for her help in the development and the preparation of the acutely dissociated nodose ganglion neurons. We also thank Dr. Carl J. Rogers for computer hardware and software implementation.

References

1. Dunlap, K., and G. Fischbach. Neurotransmitters decrease the calcium conductance activated by depolarization of embryonic chick sensory neurones. *J. Physiol. (Lond.)* 317:519–535 (1981).
2. Forscher, P., and A. S. Oxford. Modulation of calcium channels by norepinephrine in internally dialyzed avian sensory neurones. *J. Gen. Physiol.* 85:743–763 (1985).
3. Macdonald, R. L., J. H. Skerritt, and M. A. Werz. Adenosine agonists reduce voltage-dependent calcium conductance of mouse sensory neurones in culture. *J. Physiol. (Lond.)* 370:75–90 (1986).

4. Gross, R. A., and R. L. Macdonald. Dynorphin A selectively reduces a large transient (N-type) calcium current of mouse dorsal root ganglion neurons in cell culture. *Proc. Natl. Acad. Sci. USA* **84**:5469-5473 (1987).
5. Wanke, E., A. Ferroni, A. Malgaroli, A. Ambrosini, T. Pozzan, and J. Meldolesi. Activation of a muscarinic receptor selectively inhibits a rapidly inactivated Ca^{2+} current in rat sympathetic neurons. *Proc. Natl. Acad. Sci. USA* **84**:4313-4317 (1987).
6. Walker, M. W., D. A. Ewald, T. M. Perney, and R. J. Miller. Neuropeptide Y modulates neurotransmitter release and Ca^{2+} currents in rat sensory neurons. *J. Neurosci.* **8**:2438-2446 (1988).
7. Holz, G. G., IV, S. G. Rane, and K. Dunlap. GTP-binding proteins mediate transmitter inhibition of voltage-dependent calcium channels. *Nature (Lond.)* **319**:670-672 (1986).
8. Ewald, D. A., P. C. Sternweis, and R. J. Miller. Guanine nucleotide-binding protein G_i -induced coupling of neuropeptide Y receptors to Ca^{2+} channels in sensory neurons. *Proc. Natl. Acad. Sci. USA* **85**:3633-3637 (1988).
9. Gross, R. A., R. L. Macdonald, and T. Ryan-Jastrow. 2-Chloroadenosine selectively reduces the N-type calcium current of mouse dorsal root ganglion neurones in a pertussis toxin-sensitive manner. *J. Physiol. (Lond.)* **411**:585-595 (1989).
10. Gilman, A. G. G proteins and dual control of adenylate cyclase. *Cell* **36**:577-579 (1984).
11. Dolphin, A. C., and R. H. Scott. Calcium channel currents and their inhibition by (-)-baclofen in rat sensory neurones: modulation by guanine nucleotides. *J. Physiol. (Lond.)* **386**:1-17 (1987).
12. Dolphin, A. C., J. F. Wootton, R. H. Scott, and D. R. Trentham. Photoactivation of intracellular guanosine triphosphate analogues reduces the amplitude and slows the kinetics of voltage-activated calcium channel currents in sensory neurones. *Pfluegers Arch. Eur. J. Physiol.* **411**:628-636 (1988).
13. Yatani, A., J. Codina, Y. Imoto, J. P. Reeves, L. Birnbaumer, and A. M. Brown. A G protein directly regulates mammalian cardiac calcium channels. *Science (Wash. D. C.)* **238**:1288-1292 (1987).
14. Hescheler, J., W. Rosenthal, W. Trautwein, and G. Schultz. The GTP-binding protein, G_o , regulates neuronal calcium channels. *Nature (Lond.)* **325**:445-447 (1987).
15. Nowycky, M. C., A. P. Fox, and R. W. Tsien. Three types of neuronal calcium channels with different agonist sensitivity. *Nature (Lond.)* **316**:440-443 (1985).
16. Fox, A. P., M. C. Nowycky, and R. W. Tsien. Kinetic and pharmacological properties distinguishing three types of calcium currents in chick sensory neurones. *J. Physiol. (Lond.)* **394**:147-172 (1987).
17. Fox, A. P., M. C. Nowycky, and R. W. Tsien. Single channel recordings of three types of calcium channels in chick sensory neurones. *J. Physiol. (Lond.)* **394**:173-200 (1987).
18. Ikeda, S. R., G. G. Schofield, and F. F. Weight. Na^+ and Ca^{2+} currents of acutely isolated adult rat nodose ganglion cells. *J. Neurophysiol.* **55**:527-539 (1986).
19. Gross, R. A., and R. L. Macdonald. Differential actions of pentobarbitone on calcium current components of mouse sensory neurones in culture. *J. Physiol. (Lond.)* **405**:187-203 (1988).
20. Docherty, R. J. Gadolinium selectively blocks a component of calcium current in rodent neuroblastoma \times glioma hybrid (NG108-15) cells. *J. Physiol. (Lond.)* **398**:33-47 (1988).
21. Carbone, E., and H. D. Lux. Kinetics and selectivity of a low-voltage-activated calcium current in chick and rat sensory neurones. *J. Physiol. (Lond.)* **386**:547-570 (1987).
22. Carbone, E., and H. D. Lux. Single low-voltage-activated calcium channels in chick and rat sensory neurones. *J. Physiol. (Lond.)* **386**:571-601 (1987).
23. Belles, B., C. O. Malecot, J. Hescheler, and W. Trautwein. "Run-down" of the Ca current during long whole-cell recordings in guinea pig heart cells: role of phosphorylation and intracellular calcium. *Pfluegers Arch. Eur. J. Physiol.* **411**:353-360 (1988).
24. Armstrong, D., and R. Eckert. Voltage-activated calcium channels that must be phosphorylated to respond to membrane depolarization. *Proc. Natl. Acad. Sci. USA* **84**:2518-2522 (1987).
25. Chad, H., and R. Eckert. An enzymatic mechanism for calcium current inactivation in dialyzed *Helix* neurones. *J. Physiol. (Lond.)* **378**:31-51 (1986).
26. Kameyama, M., A. Kameyama, T. Nakayama, and M. Kaibara. Tissue extract recovers cardiac calcium channels from "run-down." *Pfluegers Arch. Eur. J. Physiol.* **412**:328-330 (1988).
27. Osterrieder, W., G. Brum, J. Hescheler, W. Trautwein, V. Flockerzi, and F. Hofmann. Injection of subunits of cyclic AMP-dependent protein kinase into cardiac myocytes modulates calcium current. *Nature (Lond.)* **298**:576-578 (1982).
28. Gross, R. A., M. D. Uhler, and R. L. Macdonald. Protein kinase A enhances, and ATP- γ -S reduces calcium components of rat nodose ganglion neurones. *Soc. Neurosci. Abstr.* **15**:1003 (1989).
29. Bean, B. P. Neurotransmitter inhibition of neuronal calcium currents by changes in channel voltage dependence. *Nature (Lond.)* **340**:153-156 (1989).
30. Moas, J. Signal transduction by receptor-responsive guanyl nucleotide-binding proteins: modulation by bacterial toxin-catalyzed ADP-ribosylation. *Clin. Res.* **35**:451-458 (1987).
31. Rane, S. A., and K. Dunlap. Kinase C activator 1,2-oleoylacetyl glycerol attenuates voltage-dependent calcium current in sensory neurones. *Proc. Natl. Acad. Sci. USA* **83**:184-188 (1986).
32. Cachelin, A. B., J. E. de Peyer, S. Kokubun, and H. Reuter. Ca^{2+} channel modulation by 8-bromocyclic AMP in cultured heart cells. *Nature (Lond.)* **304**:462-464 (1983).
33. Eckert, R., J. E. Chad, and D. Kalman. Enzymatic regulation of calcium current in dialyzed and intact molluscan neurones. *J. Physiol. (Paris)* **81**:318-324 (1986).
34. Hirning, L. D., A. P. Fox, G. W. McCleskey, B. M. Olivera, S. A. Thayer, R. J. Miller, and R. W. Tsien. Dominant role of N-type Ca^{2+} channels in evoked release of norepinephrine from rat sympathetic neurones. *Science (Wash. D. C.)* **239**:57-61 (1988).
35. Perney, T. M., L. D. Hirning, S. E. Leeman, and R. J. Miller. Multiple calcium channels mediate neurotransmitter release from peripheral neurones. *Proc. Natl. Acad. Sci. USA* **83**:6656-6659 (1986).

Send reprint requests to: Dr. Robert A. Gross, Neuroscience Laboratory Building, 1103 E. Huron Street, Ann Arbor, Michigan 48104.